Structural Engineering and Mechanics, *Vol. 47, No. 4 (2013) 455-470*
DOI: http://dx.doi.org/10.12989/sem.2013.47.4.455

Dynamic analysis of a beam subjected to an eccentric rolling disk

Jia-Jang Wu*

Department of Marine Engineering, College of Maritime, National Kaohsiung Marine University, No. 482,Jhongjhou 3rd Road, Cijin District, Kaohsiung City 80543, Taiwan

(Received November 4, 2011, Revised August 1, 2013, Accepted August 7, 2013)

Abstract. This paper presents a theory concerning the beam element subjected to an eccentric rolling disk (or simply called the eccentric-disk-loaded beam element) such that the dynamic responses of a beam subjected to an eccentric rolling disk with its inertia force, Coriolis force and centrifugal force considered can be easily determined. To this end, the property matrices of an eccentric-disk-loaded beam element are firstly derived by means of the Lagrange's equations. Then, the overall property matrices of the entire vibrating system are determined by directly adding the property matrices of the eccentric-disk-loaded beam element to the overall ones of the entire beam itself. Finally, the Newmark direct integration method is used to solve the equations of motion for the dynamic responses of a beam subjected to an eccentric rolling disk. Some factors relating to the title problem, such as the eccentricity, radius and rotating speed of the rolling disk, and the Coriolis force and centrifugal force induced by the rolling disk are investigated. Numerical results reveal that the influence of last factors on the dynamic responses of the pinned-pinned beam is significant except the centrifugal force.

Keywords: eccentric rolling disk; eccentricity; rotating speed; Coriolis force; centrifugal force

1. Introduction

Moving-load-induced vibration problem is an important research topic in civil and mechanical engineering. Therefore, the literature in this field is numerous. For instant, Wu and Dai (1987), Wu *et al.* (1987), Cifuentes (1989), Frỳba (1999), Wu and Chiang (2003), Kim (2005), Kidarsa (2008), Zhai and Song (2010), Bamford (2010), Cao *et al.* (2010), Charles (2010), Wu and Law (2010), and Law and Zhu (2011) have studied the dynamic characteristics of structures (e.g., beams, plates, bridges, etc.) due to moving loads by means of various analytical and numerical methods. In addition, Wu (2005) has presented the theory of moving mass element to investigate the horizontal and vertical dynamic characteristics of a portal frame under the action of a moving distributed mass. From the foregoing literature review, it is found that the effect of eccentricity of the moving mass is not considered in the existing literature. For the above reason, this paper presents a concept of *eccentric-disk-loaded beam element* such that the effect of eccentricity of the moving mass can be easily taken into consideration. To this end, the beam element subjected to an eccentric rolling disk is considered as an *eccentric-disk-loaded beam element* and then the property

*Corresponding author, Professor, E-mail: jjangwu@mail.nkmu.edu.tw

http://www.techno-press.org/?journal=sem&subpage=8 ISSN: 1225-4568 (Print), 1598-6217 (Online)

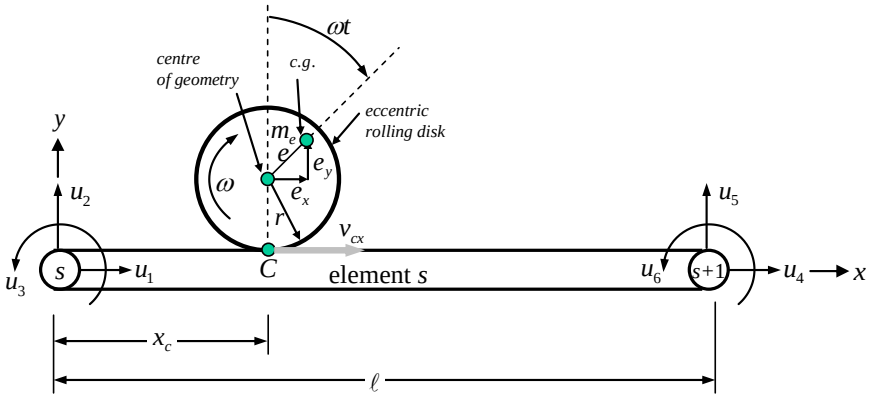

Fig. 1 A beam element subjected to an eccentric rolling disk with mass m_e

matrices of the element are derived by means of the Lagrange's equations. It has been found that, by using this concept, one can easily take account of the effects of inertia force, Coriolis force and centrifugal force of the eccentric rolling disk by directly adding the last property matrices of the *eccentric-disk-loaded beam element* to the overall ones of the entire beam itself. It is noted that the property matrices of the *eccentric-disk-loaded beam element* are dependent on the instantaneous position of the rolling disk, thus, they are time-dependent and so are the overall mass, damping and stiffness matrices of the entire vibrating system. In addition, it is assumed that the rolling disk is always in close contact with the beam, in this paper.

For validation, the dynamic responses of a pinned-pinned beam subjected to a rolling disk with eccentricity e = 0.0 m are determined and compared with those of the same beam subjected to a concentrated mass and good agreement is achieved. Some pertinent factors, such as the eccentricity, radius and rotating speed of the rolling disk, and the Coriolis force and centrifugal force induced by the rolling disk are investigated. It has been found that the influence of last parameters on the dynamic responses of the pinned-pinned beam is significant except the centrifugal force.

2. Equations of motion for the eccentric-disk-loaded beam element

Fig. 1 shows a beam element subjected to an eccentric rolling disk m_e, i.e., the eccentric-disk-loaded beam element. If, at any instant of time t, the velocities for center of gravity (c.g.) and center of geometry of the eccentric rolling disk are $\vec{v}_e$ and $\vec{v}_g$, respectively, then the following relation can be obtained.

$$\vec{v}_e = \vec{v}_g + \vec{v}_{e/g} \tag{1}$$

where $\vec{v}_{e/g}$ is the velocity of c.g., of the eccentric rolling disk relative to its center of geometry, i.e.

$$\vec{v}_{e/g} = -\omega \vec{k} \times (e_x \vec{i} + e_y \vec{j}) \tag{2}$$

In the last Eq., ω is the rotating speed of the eccentric rolling disk; $\vec{i}$, $\vec{j}$ and $\vec{k}$ are the unit vectors, in *x*, *y* and *z* directions, respectively; while e_x and e_y are respectively the distances between the geometric center and c.g., of the eccentric rolling disk in horizontal (*x*) and vertical (*y*) directions given by (cf., Fig. 1)

$$e_x = e\sin(\omega t) \tag{3a}$$

$$e_y = e\cos(\omega t) \tag{3b}$$

where *e* is the eccentricity of the rolling disk.

If the eccentric rolling disk is moving on the beam in the *x* direction and is always in close contact with the beam and without slip, one has (cf., Fig. 1)

$$\vec{v}_g = (\dot{u}_{cx} + v_{cx})\vec{i} + \dot{u}_{cy}\vec{j} \tag{4}$$

where $\dot{u}_{cx}$ and $\dot{u}_{cy}$ are the velocities of the contact point *C* between the eccentric rolling disk and the beam, due to beam vibrations, in the *x* and *y* directions, respectively, while v_{cx} is the moving speed of the eccentric rolling disk in the *x* direction.

Substituting Eqs. (2) and (4) into Eq. (1), one obtains

$$\vec{v}_e = (\dot{u}_{cx} + v_{cx} + \omega e_y)\vec{i} + (\dot{u}_{cy} - \omega e_x)\vec{j} \tag{5}$$

The kinetic energy of the eccentric rolling disk is

$$T = \frac{1}{2} m_e (\vec{v}_e \cdot \vec{v}_e) \tag{6}$$

Introducing Eq. (5) into Eq. (6) yields

$$\begin{aligned} T = {} & \frac{1}{2} m_e (\dot{u}_{cx}^2 + v_{cx}^2 + \dot{u}_{cy}^2) + \frac{1}{2}[m_e (e_x^2 + e_y^2)]\omega^2 \\ & + m_e \dot{u}_{cx} \omega e_y + m_e v_{cx} \omega e_y + m_e \dot{u}_{cx} v_{cx} - m_e \dot{u}_{cy} \omega e_x \end{aligned} \tag{7}$$

The potential energy of the eccentric rolling disk, with respect to the horizontal $\bar{x}$-axis, is

$$V = m_e g[u_{cy} + r + e\cos(\omega t)] \tag{8}$$

where u_{cy} represents the vertical displacement of the contact point *C*.

Substituting Eqs. (7) and (8) into the following Lagrange's Equations. (Clough and Penzien 1993)

$$\frac{\partial}{\partial t}\left(\frac{\partial T}{\partial \dot{u}_{cx}}\right) - \frac{\partial T}{\partial u_{cx}} + \frac{\partial V}{\partial u_{cx}} = 0 \tag{9a}$$

$$\frac{\partial}{\partial t}\left(\frac{\partial T}{\partial \dot{u}_{cy}}\right) - \frac{\partial T}{\partial u_{cy}} + \frac{\partial V}{\partial u_{cy}} = 0 \tag{9b}$$

one obtains

$$m_e\ddot{u}_{cx} + m_e\frac{d(\omega e_y)}{dt} + m_e\dot{v}_{cx} = 0 \tag{10a}$$

$$m_e\ddot{u}_{cy} - m_e\frac{d(\omega e_x)}{dt} + m_e g = 0 \tag{10b}$$

Substituting Eqs. (3a) and (3b) into Eqs. (10a) and (10b) yields

$$m_e\ddot{u}_{cx} - m_e\omega^2\, e\sin(\omega t) + m_e\dot{v}_{cx} = 0 \tag{11a}$$

$$m_e\ddot{u}_{cy} - m_e\omega^2\, e\cos(\omega t) + m_e g = 0 \tag{11b}$$

The above two expressions represent the equations of motion of the eccentric rolling disk. For the eccentric-disk-loaded beam element as shown in Fig. 1, if the effects of eccentricity and rotation of the rolling disk m_e are neglected, then the horizontal (x) and vertical (y) force components at the contact point C are respectively given by (Cifuentes 1989)

$$f_{cx,e=0} = m_e(\ddot{u}_{cx} + 2v_{cx}\dot{u}'_{cx} + v_{cx}^2 u''_{cx}) \tag{12a}$$

$$f_{cy,e=0} = m_e(\ddot{u}_{cy} + 2v_{cx}\dot{u}'_{cy} + v_{cx}^2 u''_{cy}) \tag{12b}$$

In the last expressions, $u_{cx} \equiv u_{cx}(x, t)$ and $u_{cy} \equiv u_{cy}(x, t)$, respectively, represent the horizontal (x) and vertical (y) displacements of the beam at position x and time t, while $\ddot{u}_{cx}$ represents the acceleration of the beam in the horizontal (x) direction. Moreover, $m_e\ddot{u}_{cx}$ and $m_e\ddot{u}_{cy}$, $2m_e v_{cx}\dot{u}'_{cx}$ and $2m_e v_{cx}\dot{u}'_{cy}$, and $m_e v_{cx}^2 u''_{cx}$ and $m_e v_{cx}^2 u''_{cy}$, represent the inertia forces, Coriolis forces and centrifugal forces in the horizontal (x) and vertical (y) directions, respectively, due to the rolling disk. Note that the centrifugal forces are due to the fact that the rolling disk is moving along the deformed shape of the beam.

It is evident that, if the effects of eccentricity and rotation of the rolling disk m_e as shown in Fig. 1 is considered, then the *element forces* for the eccentric-disk-loaded beam element in the x and y-directions are determined by superposing the force components appearing in Eqs. (11a) and (11b) on Eqs. (12a) and (12b), respectively, except the inertial forces $m_e\ddot{u}_{cx}$ and $m_e\ddot{u}_{cy}$ that have already been considered in Eqs. (12a) and (12b). The results are

$$f_{cx} = m_e(\ddot{u}_{cx} + 2v_{cx}\dot{u}'_{cx} + v_{cx}^2 u''_{cx}) - m_e\omega^2\, e\sin(\omega t) + m_e\dot{v}_{cx} \tag{13a}$$

$$f_{cy} = m_e(\ddot{u}_{cy} + 2v_{cx}\dot{u}'_{cy} + v_{cx}^2 u''_{cy}) - m_e\omega^2\, e\cos(\omega t) + m_e g \tag{13b}$$

Therefore, the equivalent nodal forces, f_i (i = 1 − 6), for the *eccentric-disk-loaded beam element* as shown in Fig. 1 are given by

$$f_i = \phi_i m_e(\ddot{u}_{cx} + 2v_{cx}\dot{u}'_{cx} + v_{cx}^2 u''_{cx}) - \phi_i[m_e\omega^2\, e\sin(\omega t) - m_e\dot{v}_{cx}] \quad (i = 1 \text{ and } 4) \tag{14a}$$

$$f_i = \phi_i m_e(\ddot{u}_{cy} + 2v_{cx}\dot{u}'_{cy} + v_{cx}^2 u''_{cy}) - \phi_i[m_e\omega^2\, e\cos(\omega t) - m_e g] \quad (i = 2, 3, 5, 6) \tag{14b}$$

where ϕ_i (i =1 to 6) are shape functions given by (Yang 1986)

$$\phi_1 = 1-\varsigma \tag{15a}$$

$$\phi_2 = 1-3\varsigma^2+2\varsigma^3 \tag{15b}$$

$$\phi_3 = (\varsigma-2\varsigma^2+\varsigma^3)\ell \tag{15c}$$

$$\phi_4 = \varsigma \tag{15d}$$

$$\phi_5 = 3\varsigma^2-2\varsigma^3 \tag{15e}$$

$$\phi_6 = (-\varsigma^2+\varsigma^3)\ell \tag{15f}$$

with

$$\varsigma = \frac{x_c}{\ell} \tag{16}$$

where ℓ is the length of the beam element and x_c is the distance between the location of the contact point C and the left end of the beam element, at time t, as one may see from Fig. 1.

According to the definition of shape functions and the concept of superposition, one has

$$u_{cx} = u_1\phi_1 + u_4\phi_4 \tag{17}$$

$$u_{cy} = u_2\phi_2 + u_3\phi_3 + u_5\phi_5 + u_6\phi_6 \tag{18}$$

where u_i (i =1 to 6) are the nodal displacements for the two nodes of the beam element shown in Fig. 1.

Substituting Eqs. (17)-(18) into Eqs. (14a) and (14b) and writing the resulting expressions in matrix form, one obtains

$$[m]\{\ddot{u}\}+[c]\{\dot{u}\}+[k]\{u\}+\{f_e\}=\{f\} \tag{19}$$

where

$$\{u\} = [u_1 \quad u_2 \quad u_3 \quad u_4 \quad u_5 \quad u_6]^T \tag{20}$$

$$[m] = m_e\begin{bmatrix} \phi_1\phi_1 & 0 & 0 & \phi_1\phi_4 & 0 & 0 \\ 0 & \phi_2\phi_2 & \phi_2\phi_3 & 0 & \phi_2\phi_5 & \phi_2\phi_6 \\ 0 & \phi_3\phi_2 & \phi_3\phi_3 & 0 & \phi_3\phi_5 & \phi_3\phi_6 \\ \phi_4\phi_1 & 0 & 0 & \phi_4\phi_4 & 0 & 0 \\ 0 & \phi_5\phi_2 & \phi_5\phi_3 & 0 & \phi_5\phi_5 & \phi_5\phi_6 \\ 0 & \phi_6\phi_2 & \phi_6\phi_3 & 0 & \phi_6\phi_5 & \phi_6\phi_6 \end{bmatrix} \tag{21}$$

$$[c] = 2m_e v_{cx} \begin{bmatrix} \phi_1\phi_1' & 0 & 0 & \phi_1\phi_4' & 0 & 0 \\ 0 & \phi_2\phi_2' & \phi_2\phi_3' & 0 & \phi_2\phi_5' & \phi_2\phi_6' \\ 0 & \phi_3\phi_2' & \phi_3\phi_3' & 0 & \phi_3\phi_5' & \phi_3\phi_6' \\ \phi_4\phi_1' & 0 & 0 & \phi_4\phi_4' & 0 & 0 \\ 0 & \phi_5\phi_2' & \phi_5\phi_3' & 0 & \phi_5\phi_5' & \phi_5\phi_6' \\ 0 & \phi_6\phi_2' & \phi_6\phi_3' & 0 & \phi_6\phi_5' & \phi_6\phi_6' \end{bmatrix} \tag{22}$$

$$[k] = m_e v_{cx}^2 \begin{bmatrix} \phi_1\phi_1'' & 0 & 0 & \phi_1\phi_4'' & 0 & 0 \\ 0 & \phi_2\phi_2'' & \phi_2\phi_3'' & 0 & \phi_2\phi_5'' & \phi_2\phi_6'' \\ 0 & \phi_3\phi_2'' & \phi_3\phi_3'' & 0 & \phi_3\phi_5'' & \phi_3\phi_6'' \\ \phi_4\phi_1'' & 0 & 0 & \phi_4\phi_4'' & 0 & 0 \\ 0 & \phi_5\phi_2'' & \phi_5\phi_3'' & 0 & \phi_5\phi_5'' & \phi_5\phi_6'' \\ 0 & \phi_6\phi_2'' & \phi_6\phi_3'' & 0 & \phi_6\phi_5'' & \phi_6\phi_6'' \end{bmatrix} \tag{23}$$

$$\{f_e\} = \begin{Bmatrix} -\phi_1[m_e\omega^2 e\sin(\omega t) - m_e\dot{v}_{cx}] \\ -\phi_2[m_e\omega^2 e\cos(\omega t) - m_e g] \\ -\phi_3[m_e\omega^2 e\cos(\omega t) - m_e g] \\ -\phi_4[m_e\omega^2 e\sin(\omega t) - m_e\dot{v}_{cx}] \\ -\phi_5[m_e\omega^2 e\cos(\omega t) - m_e g] \\ -\phi_6[m_e\omega^2 e\cos(\omega t) - m_e g] \end{Bmatrix} \tag{24}$$

$$\{f\} = [f_1 \quad f_2 \quad f_3 \quad f_4 \quad f_5 \quad f_6]^T \tag{25}$$

Eq. (19) is the equations of motion of the *eccentric-disk-loaded beam element*, [*m*], [*c*] and [*k*] are the mass, damping and stiffness matrices of the *eccentric-disk-loaded beam element*, respectively, $\{f_e\}$ is the external force vector induced by the eccentric rolling disk, while $\{f\}$ is the equivalent nodal force vector.

3. Equations of motion of the entire structural system

The equations of motion of a multiple-degree-of-freedom damped structural system are given by

$$[\overline{M}(t)]\{\ddot{\overline{y}}(t)\} + [\overline{C}(t)]\{\dot{\overline{y}}(t)\} + [\overline{K}(t)]\{\overline{y}(t)\} = \{\overline{F}(t)\} \tag{26}$$

In the last equation, $[\overline{M}(t)]$, $[\overline{C}(t)]$ and $[\overline{K}(t)]$ are respectively the *instantaneous* overall mass, damping and stiffness matrices; $\{\ddot{\overline{y}}(t)\}$, $\{\dot{\overline{y}}(t)\}$ and $\{\overline{y}(t)\}$ are respectively the acceleration, velocity and displacement vectors; while $\{\overline{F}(t)\}$ is the *instantaneous* external force

vector. In Eq. (26), $[\overline{M}(t)]$, $[\overline{C}(t)]$ and $[\overline{K}(t)]$ are the *instantaneous* matrices because they are composed of the *constant* overall mass and stiffness matrices of the entire beam itself and the *time-dependent* element property matrices of the *eccentric-disk-loaded beam element*. In addition, because the external force vector induced by the rolling disk m_e and its position vary with time, $\{\overline{F}(t)\}$ is also a *time-dependent* vector. The *instantaneous* overall mass matrix $[\overline{M}(t)]$, damping matrix $[\overline{C}(t)]$, stiffness matrix $[\overline{K}(t)]$ and the *instantaneous* external force vector $\{\overline{F}(t)\}$ are determined as follows:

3.1 Overall mass and stiffness matrices

In order to take the effects of inertia force and centrifugal force of the eccentric rolling disk into account, the contribution of the mass and stiffness matrices of the *eccentric-disk-loaded beam element*, (i.e., [*m*] and [*k*] respectively given by Eqs. (21) and (23)) must be added to the overall corresponding ones of the entire beam itself, $[M_b]$ and $[K_b]$, i.e.

$$[\overline{M}]_{n\times n} = [M_b]_{n\times n} + [m]_{6\times 6} \tag{27a}$$

$$[\overline{K}]_{n\times n} = [K_b]_{n\times n} + [k]_{6\times 6} \tag{27b}$$

In the last equations

$$\overline{M}_{ij} = M_{b,ij} \quad (i, j = 1 \text{ to } n) \tag{28a}$$

$$\overline{K}_{ij} = K_{b,ij} \quad (i, j = 1 \text{ to } n) \tag{28b}$$

except

$$\overline{M}_{s_i s_j} = M_{b,s_i s_j} + m_{ij} \ (i, j = 1 \text{ to } 6) \tag{29a}$$

$$\overline{K}_{s_i s_j} = K_{b,s_i s_j} + k_{ij} \ (i, j = 1 \text{ to } 6) \tag{29b}$$

In Eqs. (27)-(29), *n* is the total degrees of freedom of the entire structural system; $[M_b]$ and $[K_b]$ are respectively the overall mass and stiffness matrices of the beam itself obtained by assembling all its element mass and stiffness matrices (Przemieniecki 1985); while the subscripts s_i and s_j (i, j = 1 to 6) are the numberings for the 6 degrees of freedom of the two nodes of the beam element on which the eccentric rolling disk m_e applies at time *t*.

3.2 Overall damping matrix

Because the damping matrices of the structural elements are difficult to be found from the existing literature, the overall damping matrix $[C_b]$ of the beam is determined by using the theory of Rayleigh damping (Bathe 1982), i.e.

$$[C_b] = a[\overline{M}] + b[\overline{K}] \tag{30a}$$

with

$$a = \frac{2\omega_i\omega_j(\xi_i\omega_j - \xi_j\omega_i)}{\omega_j^2 - \omega_i^2} \tag{30b}$$

$$b = \frac{2(\xi_j\omega_j - \xi_i\omega_i)}{\omega_j^2 - \omega_i^2} \tag{30c}$$

where $[\overline{M}]$ and $[\overline{K}]$ are respectively the overall mass and stiffness matrices given by Eqs. (27a) and (27b), while ξ_i and ξ_j are damping ratios corresponding to any two natural frequencies of the structure, ω_i and ω_j.

If the Coriolis force induced by the eccentric rolling disk m_e is considered, the contribution of the damping matrix of the *eccentric-disk-loaded beam element*, (i.e., $[c]$ given by Eq. (22)) must be added to the overall damping matrix of the beam itself, $[C_b]$, to establish the *instantaneous* overall damping matrix, $[\overline{C}]$, i.e.

$$[\overline{C}]_{n\times n} = [C_b]_{n\times n} + [c]_{6\times 6} \tag{31a}$$

where

$$\overline{C}_{ij} = C_{b,ij} \qquad (i, j = 1 \text{ to } n) \tag{31b}$$

except

$$\overline{C}_{s_i s_j} = C_{b,s_i s_j} + c_{ij} \quad (i, j = 1 \text{ to } 6) \tag{31c}$$

3.3 Overall external force vector

If, at any instant of time t, the beam is subjected to an eccentric rolling disk, then all nodal forces of the beam are equal to zero except those at the two nodes of the s^{th} beam element on which the eccentric rolling disk m_e applies, i.e.

$$\{\overline{F}(t)\} = [0 \quad \cdots \quad f_1^{(s)} \quad f_2^{(s)} \quad f_3^{(s)} \quad f_4^{(s)} \quad f_5^{(s)} \quad f_6^{(s)} \quad \cdots \quad 0]^T \tag{32}$$

where $f_i^{(s)}$ (i = 1 to 6) are respectively the external force vector induced by the eccentric rolling disk given by Eq. (24). They are the s_i-th coefficients of $\{\overline{F}(t)\}$, where s_i (i = 1 to 6) are the numberings for the 6 degrees of freedom of the sth beam element on which the eccentric rolling disk m_e applies at time t. The value of x_c required by Eq. (16) is determined by

$$x_c = \bar{x}_c - (s-1)\ell \tag{33}$$

where s denotes the numbering of the beam element at which the eccentric rolling disk is located and is determined by

$$s = (\text{Integer part of } \bar{x}_c/\ell) + 1 \tag{34}$$

In Eq. (34), $\bar{x}_c$ is the global (axial) co-ordinate for the eccentric rolling disk (or contact point C), at any time t, given by

$$\bar{x}_c = \bar{x}_{c0} + v_{cx}t \tag{35}$$

with

$$v_{cx} = \omega \cdot r \tag{36}$$

where $\bar{x}_{c0}$ and v_{cx} are respectively the initial global (axial) coordinate and moving speed of the eccentric rolling disk, while ω and r are respectively the rotating speed (angular velocity) and radius of the eccentric rolling disk.

4. Vibration responses of a beam subjected to an eccentric rolling disk

If the effects of inertia force, Coriolis force and centrifugal force induced by the eccentric rolling disk are considered, then the dynamic responses of the beam subjected to the eccentric rolling disk may be obtained with the following steps:

1. Calculate the instantaneous mass, damping and stiffness matrices, [m], [c] and [k], of the *eccentric-disk-loaded beam element*, with Eqs. (21), (22) and (23).

2. Determine the *instantaneous* overall mass and stiffness matrices, $[\overline{M}]$ and $[\overline{K}]$, (see Eqs. (27)-(29)), the *instantaneous* overall damping matrix $[\overline{C}]$ (see Eqs. (30)-(31)) and the *instantaneous* overall force vector $\{\overline{F}(t)\}$ (see Eqs. (32)-(36)), at time t.

3. Determine the dynamic responses of the beam by solving for the Eqs. of motion, Eq. (26), with the Newmark direct integration method (Bathe 1982).

4. Repeat steps 1-3 to obtain the dynamic responses of the beam at time $t = t_r = t_{r-1} + \Delta t$ (with $r = 1, 2, \ldots$ and $t_0 = 0$), where Δt is the time interval.

5. Numerical results and discussions

In this section, the dimensions and physical constants for the uniform pinned-pinned beam (cf., Fig. 2) are: the cross-section is rectangular with width b = 0.018113 m and height h = 0.072322 m, the area moment of inertia $I = bh^3/12 = 5.71 \times 10^{-7}$ m^4, total length L = 4.352 m, mass density ρ = 15267.1756 kg/m^3 and Young's modulus $E = 205.9936 \times 10^8$ kg/m^2 = 2020.797216×10^8 N/m^2. Note that, for convenience of comparison, the above dimensions and material properties of the pinned-pinned beam are taken to be identical to those of Cifuentes (1989).

All the numerical results presented in this paper are obtained based on the acceleration of gravity g = 9.81 m/s^2 and the time interval $\Delta t = 0.001$ second. The overall damping matrix of the entire structural system, $[\overline{C}(t)]$, is obtained based on the lowest two natural frequencies ω_1 and ω_2 with damping ratios $\xi_1 = \xi_2 = 0.003$. Moreover, the finite element model of the beam is composed of 14 identical beam elements and 15 nodes.

5.1 Validation

Although the technique presented in this paper is developed for the dynamic analysis of a beam

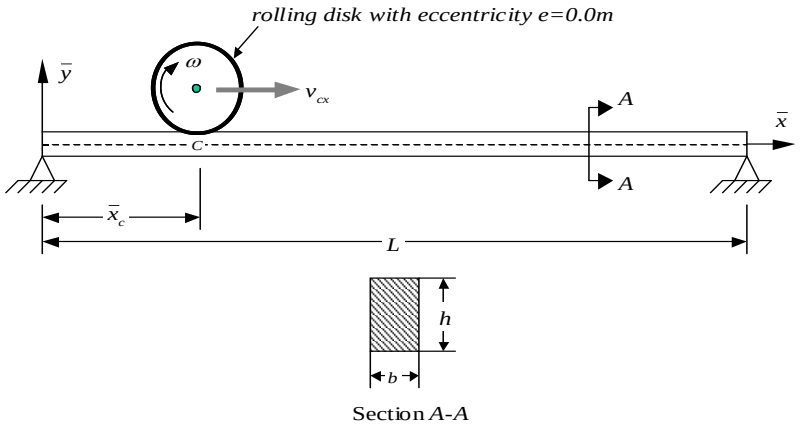

Fig. 2 A pinned-pinned beam subjected to a rolling disk with eccentricity e = 0.0 m

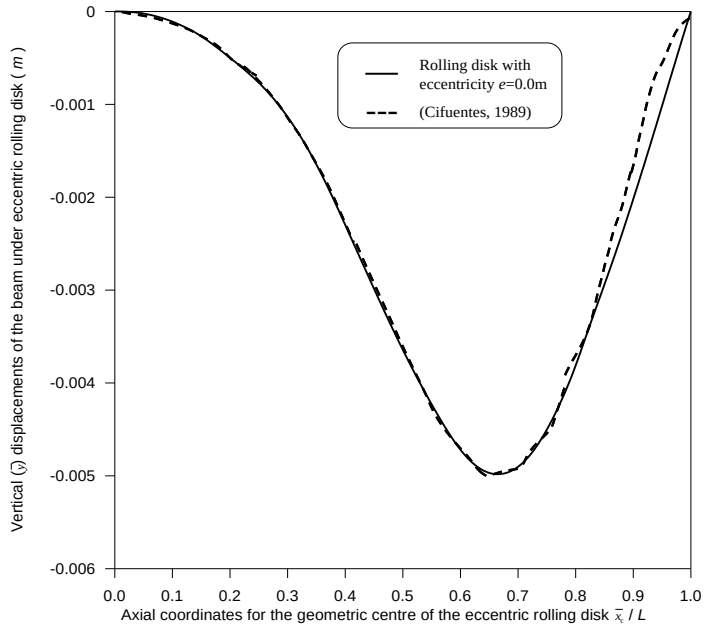

Fig. 3 Time histories for the vertical ($\bar{y}$) displacements of the beam at contacting point C of the rolling disk with eccentricity e = 0.0 m

subjected to an eccentric rolling disk, it is also available for that subjected to a concentrated mass if the magnitude of the concentrated mass is equal to the mass of the eccentric rolling disk with its eccentricity e = 0.0m. In this subsection, the pinned-pinned beam is assumed to subject a rolling disk with mass m_e = 21.8 kg, eccentricity e = 0.0m and constant moving speed v_{cx} = 27.49 m/s. Then, the computer programs developed for this paper are validated by comparing the dynamic responses of the beam with those of the existing literature (Cifuentes 1989).

Fig. 3 shows the time histories for the vertical ($\bar{y}$) displacements of the contact point C between the rolling disk (with eccentricity e = 0.0m) and the beam. In the figure, the solid curve

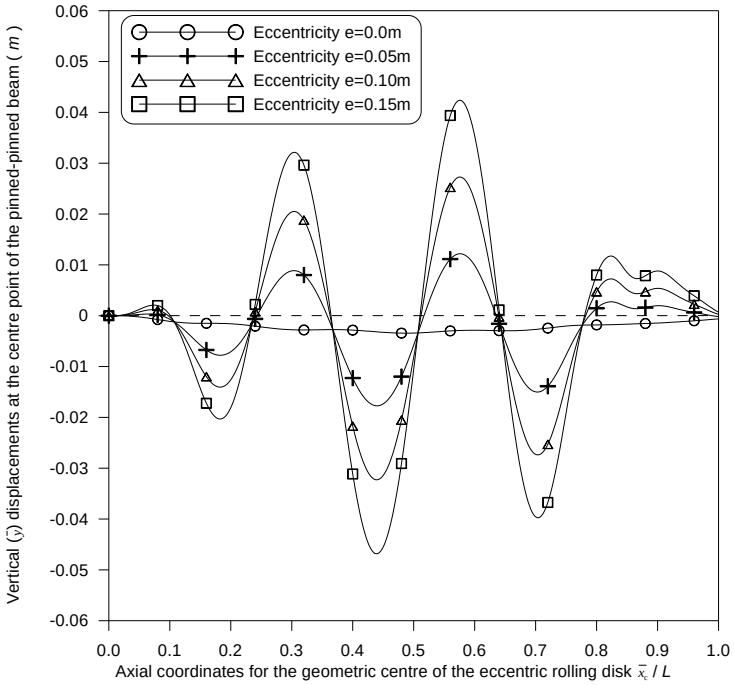

Fig. 4 Influence of eccentricity e of the rolling disk on the time histories for the vertical ($\bar{y}$) central displacements of the pinned-pinned beam

(—) represents the vertical ($\bar{y}$) displacements obtained by using the presented theory of *eccentric-disk-loaded beam element*, while the dashed curve (----) represents those obtained from Cifuentes (1989). It is evident that the differences between the last two curves are negligible.

5.2 Influence of eccentricity of the rolling disk

In this subsection, the dynamic responses of a pinned-pinned beam subjected to a rolling disk with mass m_e = 21.8 kg, radius r = 0.2 m, moving speed v_{cx} = 4.352 m/s (or rotating speed $\omega = v_{cx}/r$ = 4.352/0.2 = 21.76 rad/s) and eccentricity e = 0.0, 0.05, 0.1 or 0.15m are studied. The rolling disk is moving from left end to right end of the beam (cf., Fig. 2) and, in each case, the initial position of the eccentric mass (m_e) of the rolling disk is on the vertical line passing through left end of the beam with e_x = 0.0m and $e_y = e$ = 0.0, 0.05, 0.1 or 0.15m (cf., Fig. 1). Because the moving speed v_{cx} (or rotating speed ω) of the rolling disk is constant, the horizontal acceleration $\dot{v}_{cx}$ of the rolling disk is equal to zero. Thus, it can be seen from Eq. (24) that the larger the value of eccentricity e of the rolling disk, the larger the external force vector $\{f_e\}$ induced by the eccentric rolling disk, and also the larger the vibration responses of the pinned-pinned beam induced by eccentric rolling disk.

Fig. 4 shows the time histories for the vertical ($\bar{y}$) central displacements of the pinned-pinned beam. In the figure, the solid curves with circles (—○—), crosses (—+—),triangles (—△—) and rectangles (—□—) are the vertical ($\bar{y}$) central displacements of the pinned-pinned beam corresponding to eccentricities e = 0.0, 0.05, 0.1 and 0.15 m, respectively. From the figure, it can

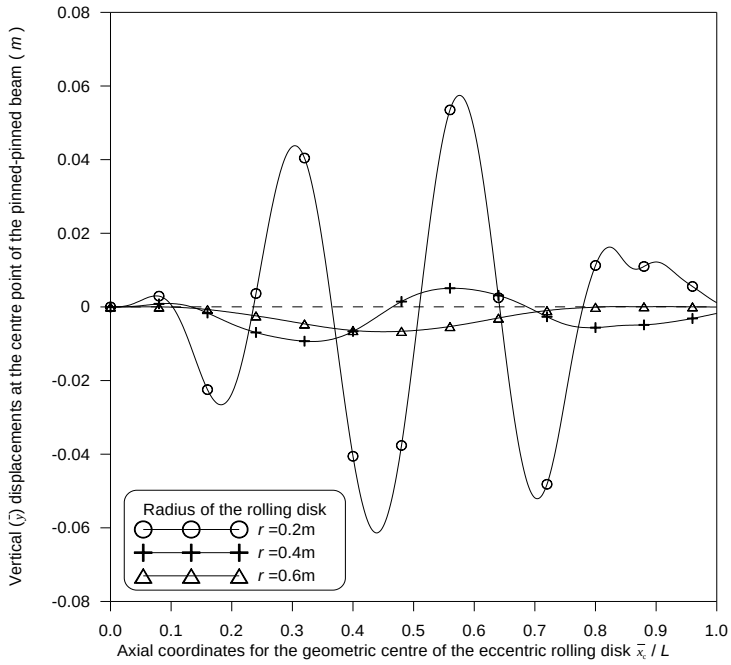

Fig. 5 Influence of disk radius r on the time histories for the vertical ($\bar{y}$) central displacements of the pinned-pinned beam

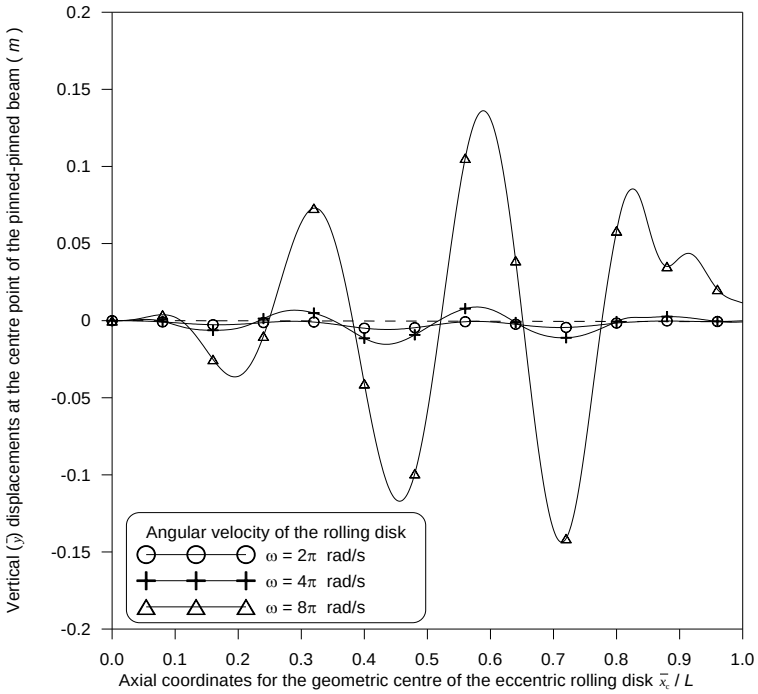

Fig. 6 Influence of rotating speed (angular velocity) ω of the rolling disk on the time histories for the vertical ($\bar{y}$) central displacements of the pinned-pinned beam

be seen that the larger the value of eccentricity e, the larger the vibration responses of the pinned-pinned beam, as expected.

5.3 Influence of radius of the eccentric rolling disk

In this subsection, the pinned-pinned beam subjected to a rolling disk with mass m_e = 21.8 kg, eccentricity e = 0.2 m, constant moving speed v_{cx} = 4.352 m/s and radius r = 0.2, 0.4 or 0.6 m is studied. From Eq. (36), one sees that $\omega = v_{cx}/r$. Thus, the rotating speeds of the rolling disk with r = 0.2, 0.4 and 0.6 m are found to be $\omega = v_{cx}/r$ = 21.76, 10.88 and 7.2533 m/s, respectively. From the above descriptions, it is evident that the larger the disk radius r, the smaller the rotating speed ω of the rolling disk. Thus, the larger the disk radius r, the smaller the external force vector $\{f_e\}$ induced by the eccentric rolling disk, as one may see from Eq. (24), and so that the smaller the vertical ($\bar{y}$) central displacements of the pinned-pinned beam induced by eccentric rolling disk.

The time histories for the vertical ($\bar{y}$) central displacements of the pinned-pinned beam are shown in Fig. 5, where the solid curves with circles (—◯—), crosses (—+—) and triangles (—△—) are respectively for the cases of r = 0.2, 0.4 and 0.6 m. Clearly, the larger the disk radius r, the smaller the vertical ($\bar{y}$) central displacements of the pinned-pinned beam induced by eccentric rolling disk, as it should be.

5.4 Influence of angular velocity of the rolling disk

All the physical parameters for the beam and rolling disk of the current example are exactly the same as those of the last example except that the disk radius r = 0.2 m is a constant and the rotating speed of the disk is $\omega = 2\pi$, 4π or 8π rad/s (or the moving speed of the rolling disk $v_{cx} = \omega \cdot r = 0.4\pi$, 0.8π or 1.6π m/s, according to Eq. (36)). From the preceding descriptions and Eq. (24), one can conclude that the larger the rotating speed ω of the eccentric rolling disk, the larger the external force vector $\{f_e\}$ induced by the disk and the larger the vertical ($\bar{y}$) central displacements of the pinned-pinned beam. It is obvious that the time histories for the vertical ($\bar{y}$) central displacements of the pinned-pinned beam shown in Fig. 6 agree with the last conclusion. In which, the solid curve with circles (—◯—) is for the case of $\omega = 2\pi$ rad/s, the one with crosses (—+—) is for the case of $\omega = 4\pi$ rad/s ,while the one with triangles (—△—) is for the case of $\omega = 8\pi$ rad/s.

5.5 Influence of Coriolis force

Since the Coriolis force induced by the eccentric rolling disk is to appear in the damping matrix $[c]$ of the *eccentric-disk-loaded beam element*, as one may see from the formulations of section 2, the effect of Coriolis force is dependent on whether or not the damping matrix $[c]$ is equal to zero. In other words, $[c] \neq 0$ is for the cases with effect of Coriolis force considered and $[c] = 0$ otherwise.

In this subsection, all physical parameters of the beam and the rolling disk are exactly the same as those of the last example. Fig. 7 shows the time histories of vertical ($\bar{y}$) central displacements of the pinned-pinned beam. In the figure, the vertical ($\bar{y}$) dynamic responses of the pinned-pinned beam with the Coriolis force *considered* (i.e., $[c] \neq 0$) are represented by the solid curves (—) and those with the Coriolis force *neglected* (i.e., $[c] = 0$) by the dashed curves (------). From Figs. 7(a)-7(c), one sees that the influence of Coriolis force on the vertical ($\bar{y}$) central displacements of

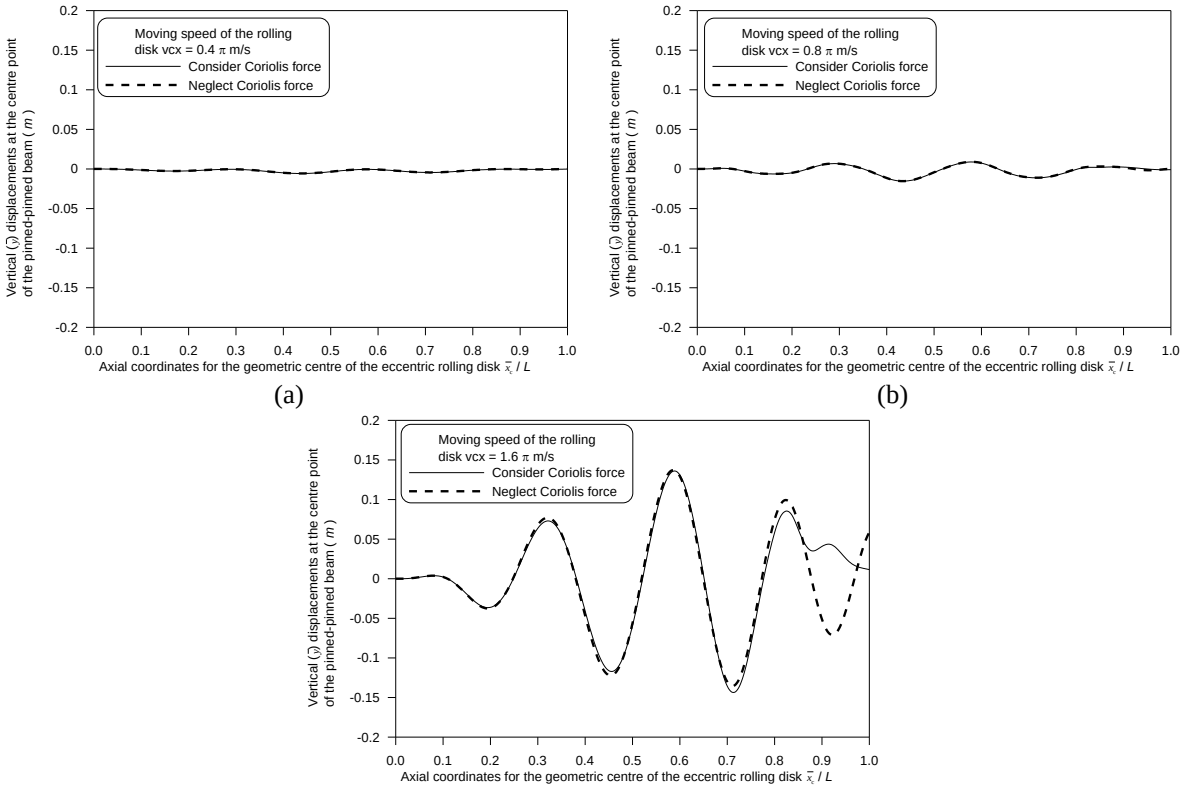

Fig. 7 Influence of *Coriolis force* of the rolling disk on the time histories for the vertical ($\bar{y}$) central displacements of the pinned-pinned beam: (a) $v_{cx} = 0.4\pi$ m/s, (b) $v_{cx} = 0.8\pi$ m/s and (c) $v_{cx} = 1.6\pi$ m/s (or rotating speeds $\omega = 2\pi$, 4π and 8π rad/s with disk radius $r = 0.2$ m)

the pinned-pinned beam increases with the increase of moving speed v_{cx} of the rolling disk. This is a reasonable result because the magnitude of the Coriolis force appearing in the damping matrix [c] of the *eccentric-disk-loaded beam element* (cf. Eq. (22)) is proportional to the moving speed v_{cx} of the rolling disk. In spite of the fact that the difference between the time histories with Coriolis force considered and neglected is not significant for the current example, its effect may be significant for other cases. Thus, it is better to take account of the effect of Coriolis force in all cases.

5.6 Influence of centrifugal force

From the formulations of section 2, one sees that the effect of centrifugal force induced by the eccentric rolling disk is reflected by the stiffness matrix [k] of the *eccentric-disk-loaded beam element*. Thus, one of the simplest ways for neglecting the effect of centrifugal force is to set [k] = [0]. The example studied here is exactly the same as that of the last subsection. Fig. 8 shows the time histories of vertical ($\bar{y}$) central displacements of the pinned-pinned beam. In which, the solid curves (—) represent the vertical ($\bar{y}$) dynamic responses of the pinned-pinned beam with the

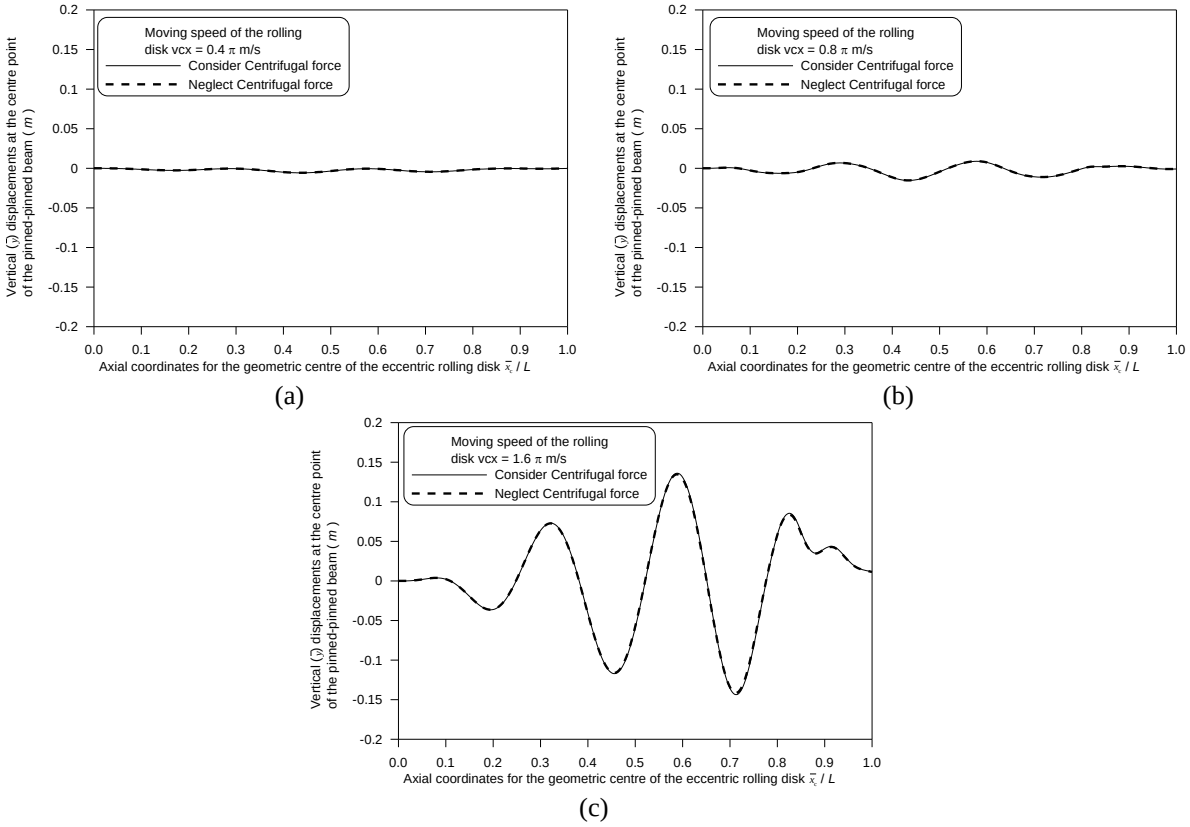

Fig. 8 Influence of *Centrifugal force* of the rolling disk on the time histories for the vertical ($\bar{y}$) central displacements of the pinned-pinned beam: (a) $v_{cx} = 0.4\pi$ m/s, (b) $v_{cx} = 0.8\pi$ m/s and (c) $v_{cx} = 1.6\pi$ m/s (or rotating speeds $\omega = 2\pi$, 4π and 8π rad/s with disk radius $r = 0.2$ m)

centrifugal force considered (i.e., $[k] \neq 0$), while the dashed curves (------) represent those with centrifugal force neglected (i.e., $[k] = 0$). In which, Figs. 8(a), 8(b) and 8(c) are respectively for the cases of moving speeds $v_{cx} = 0.4\pi$, 0.8π and 1.6π m/s (or rotating speeds $\omega = 2\pi$, 4π and 8π rad/s with disk radius $r = 0.2$ m). From the last figures, it is found that the influence of centrifugal force on the vertical ($\bar{y}$) central displacements of the pinned-pinned beam is not important for the current example. However, the above effect may be significant for other cases. Thus, it is better to consider the effect of centrifugal force in all cases for achieving satisfactory results.

6. Conclusions

This paper presents a theory of *eccentric-disk-loaded element* such that the dynamic responses of a beam subjected to an eccentric rolling disk with its inertia force, Coriolis force and centrifugal force considered can be easily obtained. Because the external force vector $\{f_e\}$ induced by the eccentric rolling disk is proportional to the eccentricity e and rotating speed ω of the rolling disk, the larger the eccentricity e and rotating speed ω of the rolling disk, the larger the vibration

responses of the pinned-pinned beam subjected to the eccentric rolling disk. If the horizontal speed v_{cx} and eccentricity e of the rolling disk are kept constant, then the larger the disk radius r, the smaller the external force vector $\{f_e\}$ induced by the eccentric rolling disk and the smaller the vertical ($\bar{y}$) central displacements of the pinned-pinned beam. Since the influence of Coriolis force on the vertical ($\bar{y}$) central displacements of the pinned-pinned beam increases with increasing the moving speed of the rolling disk, this effect should be considered in all cases to assure that better results will be achieved. Although the influence of centrifugal force on the vertical ($\bar{y}$) central displacements of the pinned-pinned beam is negligible for the example studied in this paper, this effect should be taken into consideration when the deflection of beam is larger (e.g., a long-span beam subjected to a heavy eccentric rolling disk) so that the effect of centrifugal force is significant.

References

Bamford, K. (2010), *Moving loads on railway underbridges, including: diagrams of bending moments and shearing forces and tables of equivalent uniform live loads*, Nabu Press.

Bathe, K.J. (1982), *Finite element procedures in engineering analysis*, Prentice-Hall.

Cao, Y.M., Xia, H. and Lombaert, G. (2010), "Solution of moving-load-induced soil vibrations based on the Betti–Rayleigh Dynamic Reciprocal Theorem", *Soil Dynamics and Earthquake Engineering*, **30**, 470-480.

Charles, M. (2010), *Notes on the theory of structure: reactions, moments, shears, moving loads, beams, girders, simple trusses*, ISBN: 1990001215382.

Cifuentes, O. (1989), "Dynamic response of a beam excited by a moving mass", *Finite Elements in Analysis and Design*, **5**, 237-246.

Clough, R.W. and Penzien, J. (1993), *Dynamics of structures*, McGraw-Hill.

Frỳba, L. (1999), *Vibration of Solids and Structures under Moving Loads*, Thomas Telford Ltd.

Kidarsa, A., Scott, M.H. and Higgins, C.C. (2008), "Analysis of moving loads using force-based finite elements", *Finite Elements in Analysis and Design*, **44**, 214-224.

Kim, S.M. (2005), "Stability and dynamic response of Rayleigh beam–columns on an elastic foundation under moving loads of constant amplitude and harmonic variation", *Engineering Structures*, **27**, 869-880.

Law, S.S. and Zhu, X.Q. (2011), *Moving Loads – Dynamic Analysis and Identification Techniques*, CRC Press.

Przemieniecki, J.S. (1985), *Theory of matrix structural analysis*, McGraw-Hill.

Wu, J.J. (2005), "Vibration analyses of a portal frame under the action of a moving distributed mass using moving mass element", *International Journal for Numerical Methods in Engineering*, **62**, 2028-2052.

Wu, S.Q. and Law, S.S. (2010), "Moving force identification based on stochastic finite element model", *Engineering Structures*, **32**, 1016-1027.

Wu, J.S. and Dai, C.W. (1987), "Dynamic responses of multispan nonuniform beam due to moving loads", *Journal of Structural Engineering*, **113**, 458-474.

Wu, J.S., Lee, M.L. and Lai, T.S. (1987), "The dynamic analysis of a flat plate under a moving load by the finite element method", *Journal for Numerical Methods in Engineering*, **24**, 743-762.

Wu, J.S. and Chiang, L.K. (2003), "Out-of-plane responses of a circular curved Timoshenko beam due to a moving load", *International Journal of Solids and Structures*, **40**, 7425-7448.

Yang, T.Y. (1986), *Finite Element Structural Analysis*, Prentice-Hall Inc.

Zhai, W. and Song, E. (2010), "Three dimensional FEM of moving coordinates for the analysis of transient vibrations due to moving loads", *Computers and Geotechnics*, **37**, 164-174.